Hypervelocity Impact Study for Migration from Kevlar® KM2® 705 to KM2® Plus 775

Material property measurement and evaluation as a ballistic enhancement in Whipple shields

Joshua E. Miller, Ph.D.
University of Texas at El Paso, El Paso, Texas
Johnson Space Center, Houston, Texas

Robert J. McCandless
Jacobs, Johnson Space Center, Houston, Texas

Bruce (Alan) Davis
Jacobs, Johnson Space Center, Houston, Texas

September 2021

NASA STI Program Report Series

The NASA STI Program collects, organizes, provides for archiving, and disseminates NASA's STI. The NASA STI program provides access to the NTRS Registered and its public interface, the NASA Technical Reports Server, thus providing one of the largest collections of aeronautical and space science STI in the world. Results are published in both non-NASA channels and by NASA in the NASA STI Report Series, which includes the following report types:

- TECHNICAL PUBLICATION. Reports of completed research or a major significant phase of research that present the results of NASA Programs and include extensive data or theoretical analysis. Includes compilations of significant scientific and technical data and information deemed to be of continuing reference value. NASA counterpart of peer-reviewed formal professional papers but has less stringent limitations on manuscript length and extent of graphic presentations.

- TECHNICAL MEMORANDUM. Scientific and technical findings that are preliminary or of specialized interest, e.g., quick release reports, working papers, and bibliographies that contain minimal annotation. Does not contain extensive analysis.

- CONTRACTOR REPORT. Scientific and technical findings by NASA-sponsored contractors and grantees.

- CONFERENCE PUBLICATION. Collected papers from scientific and technical conferences, symposia, seminars, or other meetings sponsored or co-sponsored by NASA.

- SPECIAL PUBLICATION. Scientific, technical, or historical information from NASA programs, projects, and missions, often concerned with subjects having substantial public interest.

- TECHNICAL TRANSLATION. English-language translations of foreign scientific and technical material pertinent to NASA's mission.

Specialized services also include organizing and publishing research results, distributing specialized research announcements and feeds, providing information desk and personal search support, and enabling data exchange services.

For more information about the NASA STI program, see the following:

- Access the NASA STI program home page at http://www.sti.nasa.gov

- Help desk contact information:

https://www.sti.nasa.gov/sti-contact-form/

and select the "General" help request type.

NASA/TM–20210020869

Hypervelocity Impact Study for Migration from Kevlar® KM2® 705 to KM2® Plus 775

Material property measurement and evaluation as a ballistic enhancement in Whipple shields

Joshua E. Miller, Ph.D.
University of Texas at El Paso, El Paso, Texas
Johnson Space Center, Houston, Texas

Bruce (Alan) Davis
Jacobs, Johnson Space Center, Houston, Texas

Robert J. McCandless
Jacobs, Johnson Space Center, Houston, Texas

Acknowledgments

This report is available in electronic form at

http://

Abstract

Dupont™, the manufacturer of Kevlar®, has begun migrating from KM2® to KM2® Plus for ballistic textiles. Kevlar® KM2® has become an essential element of numerous meteoroid and orbital debris (MMOD) shield systems primarily as a multi-layer insulation (MLI) enhancement, and as such, the migration has implications for numerous system level risk assessments for future vehicles that will need to use the newer KM2® Plus fiber system. While the chemical makeup of the two fabrics are identical, differences in processing have yielded higher tenacities and toughness for the KM2® Plus system. To address this migration, the Hypervelocity Impact Technology (HVIT) group in NASA Exploration Sciences at Johnson Space Center (JSC) has worked with the NASA Engineering and Safety Center (NESC), the Multi-Purpose Crew Vehicle (MPCV) and the MPCV European Service Module (MPCV-ESM) group of the European Space Agency (ESA) with its contractors Airbus and Thales Alenia Space-Italy (TAS-I) to study how KM2® Plus in the woven form of 850 denier 775 compares with KM2® in the woven form of 850 denier 705. The two forms of Kevlar® fabrics have been compared by direct-impact with a known mass and as the rear wall in Whipple shields using the two-stage, light-gas-gun at the Remote Hypervelocity Test Laboratory (RHTL) of NASA JSC White Sands Test Facility (WSTF). From these examinations, it has been found that KM2® Plus does in fact improve the ballistic performance as a ballistic enhancement of MLI with an estimated improvement of 9.5±6.1% between the two fabrics, and on a mass basis, the estimated mass of KM2® Plus 775 is 3.6±0.7% lighter than KM2 705, which means the mass performance improvement is even higher.

Introduction

Kevlar® a synthetic, aromatic polyamide fiber was developed for use in applications that require high strength, high modulus, toughness and thermal stability with low weight [1]. Kevlar® consists of poly(para-phenylene terephthalamide) molecules that are highly aligned and cross-linked with strong covalent bonds in chains and hydrogen bonds to form sheets [1, 2]. These sheets stack under hydrogen and van der Waals bonds and are spun together to form fibers. The collection of numerous covalent, hydrogen and van der Waals bonds per monomer results in the high tenacity and flexibility that have been leveraged for many aerospace applications.

While numerous Kevlar® fiber systems are available with varying processing conditions, Kevlar® KM2® being a moderately high modulus and moderate strength and strain limit fiber has been selected for numerous meteoroid and orbital debris (MMOD) shield systems [3]. These fibers are spun together to form yarns of varying denier that are woven into fabrics primarily as an enhancement in Multi-Layer Insulation (MLI) blankets that are part of a Whipple shield. In particular, the Kevlar® KM2® 705 fabric at 850 denier have been widely deployed in the past [3]; however, as Kevlar® KM2® is being replaced by Kevlar® KM2® Plus [4], this migration has implications for numerous system level risk assessments for future vehicles that will need to use the newer fiber system. To this end, Kevlar® KM2® Plus 775 fabric, also at 850 denier, has been chosen as the replacement for Kevlar® KM2® 705.

One vehicle that straddles this migration is the Multi-Purpose Crew Vehicle (MPCV) [5]. In early design phases, MPCV prepared to use Kevlar® KM2® 705 in rear walls of some shields, but MPCV will be assembled and operational post-migration using Kevlar® KM2® Plus 775. In the case of MPCV, the Kevlar® blanket is implemented as a component of a MLI blanket in the European Space Agency provided Service Module (MPCV-ESM) to enhance ballistic protection of

propulsion systems and avionics components [6]. To address this migration for MPCV and other NASA and ESA programs, the Hypervelocity Impact Technology (HVIT) group of NASA Astromaterials Research and Exploration Sciences at Johnson Space Center (JSC) has worked with the NASA Engineering and Safety Center (NESC), the MPCV program office and European Space Agency (ESA) with its prime contractors Airbus and Thales Alenia Space-Italy (TAS-I) to study how KM2® Plus 775 compares with KM2® 705.

The examination of the two forms of Kevlar® fabric for NESC and interested MPCV systems design teams have used two different experimental approaches: the first is by direct-impact of five layers of each fabric type with a known mass [7], and the second is by using the respective fabrics in their usual configuration of a double-wall shield [8, 9]. For both approaches, the two-stage, light-gas-gun at the Remote Hypervelocity Test Laboratory (RHTL) of NASA JSC White Sands Test Facility (WSTF) has been used to accelerate spherical particles to representative orbital speeds. This research paper reviews the materials and methods used to evaluate the two different fabrics at space environment relevant conditions both for direct-impacts and as a rear wall in a double-wall shield, discusses the analysis performed to interpret these results and provides conclusions on overall relative performance.

Materials and Methods

This effort has performed direct comparisons between Kevlar® KM2® 705 fabric 850 denier and Kevlar® KM2® Plus 775 fabric 850 denier. The Kevlar® KM2® 705 fabric has either been acquired directly from Dupont™ via TAS-I or through Hexcel® as a third-party vendor; similarly, the Kevlar® KM2® Plus 775 fabric has either been acquired directly from Dupont™ via TAS-I or through JPS Composite Materials® as a third-party distributor. In all cases the fabrics provided by TAS-I have been sealed with CS-898 water repellant, while those from distributors had no sealant applied. The masses of KM2® 705 and KM2® Plus 775 fabrics have been verified to be 0.02391±0.00011 g/cm^2 and 0.02309±0.00011 g/cm^2, respectively.

While the fabrics have been obtained through a third-party, the fibers have all been manufactured by Dupont™ using their standard techniques for the fibers. In Table 1, the technical reference properties for the fibers from Hexcel® for KM2® 705 [10] and from JPS Composite Materials for KM2® Plus 775 are reproduced [11]. As can be seen numerous properties between the two fiber types are expected to be similar with the notable exception that the KM2® Plus 775 has an approximately 8% higher tensile modulus and 8.6% higher strain to failure than KM2® 705.

Table 1 Summary of third-party distributor reference fiber properties

Fiber	Density	Tensile Strength	Tensile Modulus	Strain to Failure	Decomp. Temp.
	(g/cm^3)	(GPa)	(GPa)	(%)	(°C)
Kevlar® KM2® 850 denier	1.44	3.4	75	3.5	450
Kevlar® KM2® Plus 850 denier	1.44	3.4	81	3.8	450

On the macro level of yarns and fabric, the reference values reported by the distributors are summarized in Table 2. Hexcel® has given differing reference values of KM2® 705 [12] and both are reproduced in Table 2. The count of yarns in both the warp and fill direction are identical between the two fabric types; however, the other properties like weight, thickness and breaking strength are either equal or higher for KM2® 705 than KM2® Plus 775 depending on the reference. It is noted that the measured weights of the KM2® 705 fabric used for this work is approximately

2

the mean of the two values given by Hexcel®, and the measured weight of the KM2® Plus 775 fabric matches the value given by JPS Composite Materials®.

Table 2 Summary of third-party distributor reference fabric properties

Fiber	Style	Count		Weight		Thickness		Break Strength	
		Warp	Fill					Warp	Fill
				(oz/y^2)	(g/m^2)	(mils)	(mm)	(lb$_f$/in)	(lb$_f$/in)
Kevlar® KM2® 850 denier	705	31	31	6.9	234	13.8	0.35	899	984
Kevlar® KM2® 850 denier	705	31	31	7.2	244	12.0	0.30	880	950
Kevlar® KM2® Plus 850 denier	775	31	31	6.8	231	11.8	0.30	880	950

While the manufacturer, distributor and even other users have published values for these fabrics, the use of the Kevlar® fabrics against MMOD is highly unique relative to normal terrestrial uses. As these fabrics are being impacted by materials moving at speeds of several kilometers per second, the ability for the material to react to the forces generated by the impact is significantly different than measurements conducted on the order of or well below the material sound speeds. To this end, the fabrics have been studied separately facing impact speeds in the range of a few kilometer per second for direct-impact and at several kilometers per second as a component of double-wall shields.

Direct-Impact Experiments

To evaluate the fabrics, targets of both KM2® 705 and KM2® Plus 775 fabrics have been developed. The targets each consisted of five layers of 15 cm x 15 cm Kevlar® sheets that are secured loosely between two frames and separated by 5 cm from a witness plate of 1.0 mm Al2024-T3 as shown schematically in Figure 1a. The two securing frames are also 15 cm x 15 cm with an inner opening of 10 cm x 10 cm to expose the Kevlar® sheets. The frames are held relative to the witness plate by way of threaded rods, spacers and locking nuts with a representative target image in Figure 1b. Kevlar® sheets and witness plates are single use.
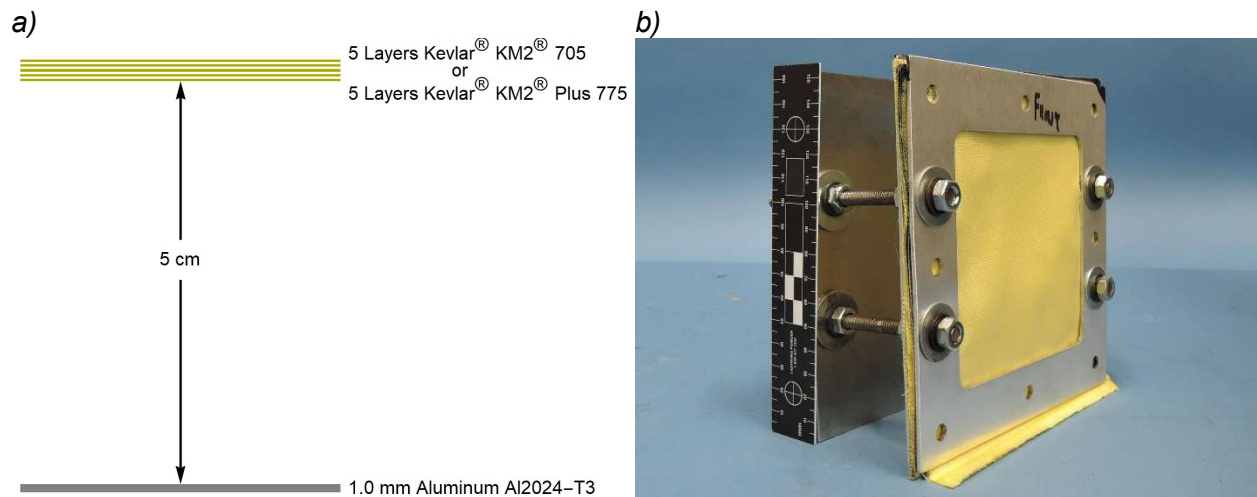
a)

5 Layers Kevlar® KM2® 705
or
5 Layers Kevlar® KM2® Plus 775

5 cm

1.0 mm Aluminum Al2024−T3

b)

Figure 1 Target images a) scaled representation and b) image of actual target with supporting hardware.

The objective for the direct-impacts into the Kevlar® is to stop a known projectile within the five layers that make up the target. To keep the majority of the impact response within the Kevlar® and incur minimal material transition in the projectile, martensitic, 440C stainless steel balls are used throughout the direct-impact testing. These steel balls are high chromium and carbon steel alloys with high hardness and toughness. As a result of the higher mass percentage of carbon (0.95-1.20%), the 440C stainless steel balls have a lower density for steel alloys around 7.67 g/cm^3. In these material property measurement experiments, the size of the SS440C projectiles have been adjusted along with the impact speeds as summarized in Table 3. All of the impacts are with SS440C projectiles impacting the Kevlar® targets normal to their surface.

Table 3 Direct-impact results matrix for Kevlar® property measurement [7]

Test Number	Fabric	Projectile Diameter (mm)	Projectile Mass (g)	Impact Speed (km/s)	Damage Measurements (mm)
HITF20356	775	0.31	0.00012	4.15	L1 = 0.36 x 0.30 perforation L2 = 0.55 x 0.46 perforation L3 = 0.60 x 0.60 perforation L4 = 0.60 x 0.40 perforation L5 = 1.30 x 0.30 perforation
HITF20357	775	0.25	0.00006	3.46	L1 = 0.37 x 0.33 perforation L2 = 0.46 x 0.43 perforation L3 = 0.43 x 0.34 perforation L4 = 0.43 x 0.36 perforation L5 = crater (1 severed, 1 in-tact)
HITF20358	705	0.25	0.00006	3.40	L1 = 0.34 x 0.33 perforation L2 = 0.36 x 0.17 perforation L3 = 0.37 x 0.29 perforation L4 = 0.46 x 0.26 perforation L5 = 0.31 x 0.21 perforation
HITF20359	775	0.43	0.00032	2.02	L1 = 0.50 x 0.20 perforation L2 = 0.40 x 0.30 perforation L3 = 0.29 x 0.25 perforation L4 = 0.35 x 0.26 perforation L5 = 0.80 x 0.20 perforation

In Table 3, the four direct-impact experiments consisted of one into KM2® 705 and three into the KM2® Plus 775 owing to the forward facing importance of the newer fabric. The single impact experiment with KM2® 705 is at 3.40 km/s with a 0.25 mm SS440C projectile. The recorded damage into each layer of Kevlar® is recorded in the table from L1 (first layer to be hit) to L5 (last layer to be hit). Micrographs of the front and back of each of the Kevlar® layers HITF20358 is shown in Figure 2 with the fronts of the fabric in Figure 2a and the back in Figure 2b. In HITF20358, all five layers of Kevlar® are perforated.
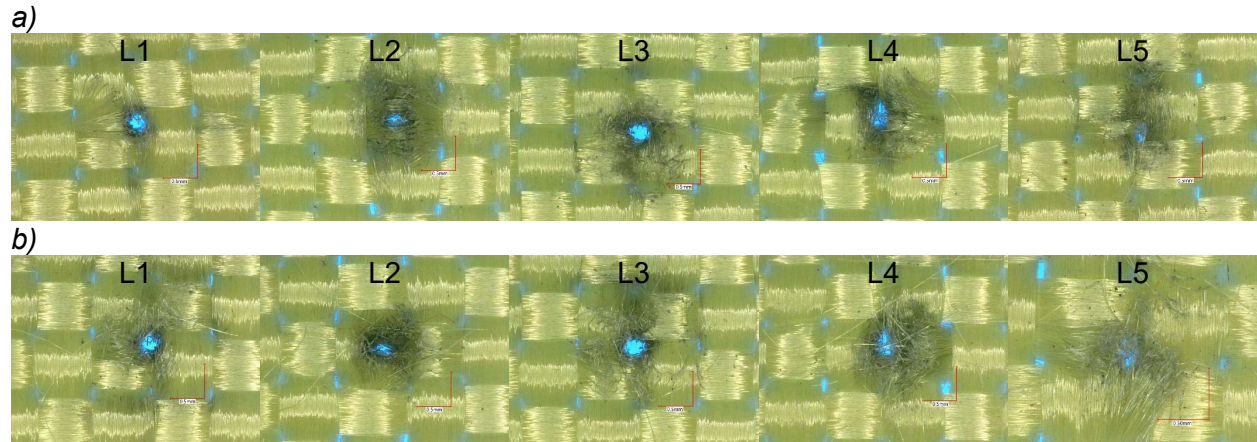
4

Figure 2 HITF20358 a) front side image of the KM2® 705 layers and b) corresponding back side images. Holes in the fabric are backlit by blue light. Each image from L1 to L5 corresponds to the order of the Kevlar® in the stack. The scale in the images is 0.50 mm.

The comparison impact experiment to HITF20358 is HITF20357 where KM2® Plus 775 has been impacted at 3.46 km/s with a 0.25 mm SS440C projectile. As done in Figure 2, the recorded damage micrographs into each layer of Kevlar® are shown for HITF20357 in Figure 3. In HITF20357, the fifth layer of Kevlar® remained in-tact; however, the force of stopping the momentum of projectile spread the yarns in the weave exposing gaps away from the yarns where debris can pass through the fabric.
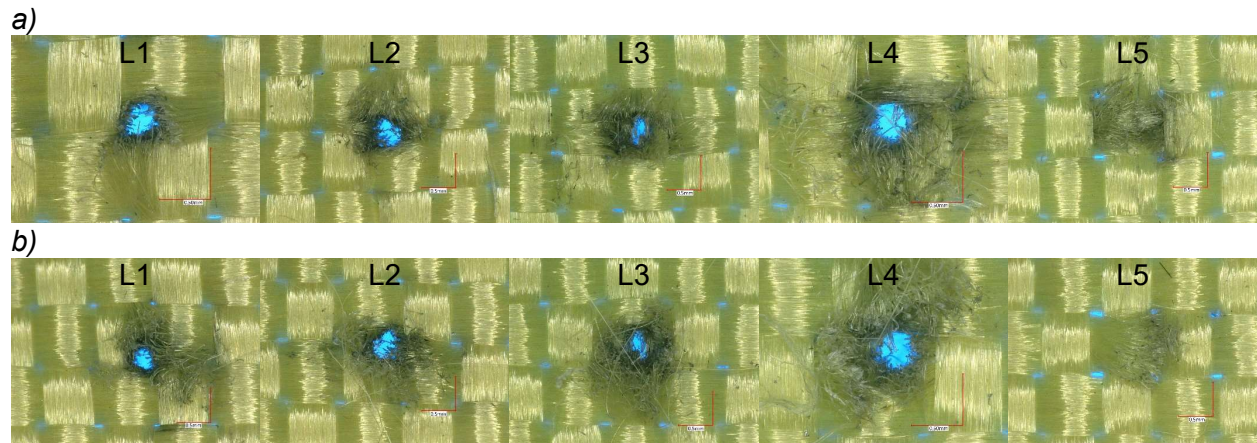
a)

b)

Figure 3 HITF20357 a) front side image of the KM2® Plus 775 layers and b) corresponding back side images. Holes in the fabric are backlit by blue light. Each image from L1 to L5 corresponds to the order of the Kevlar® in the stack. The scale in the images is 0.50 mm.

To provide a direct comparison of what passed through the Kevlar®, the witness plates for both HITF20358 and HITF20357 are shown in Figure 4. As can be seen in Figure 4a, the debris that went through the Kevlar® in HITF20358 is largely limited to a single particle that formed an 0.5 mm diameter crater of 0.25 mm depth in the Al2024-T3 witness. This crater produced a subtle 0.02 mm bump on the rear surface of the witness plate. The remnant particle in HITF20358 did not create a discernable feature on the back of the witness plate. This compares to the witness plate of HITF20357 shown in Figure 4b where two craters formed with the most significant also being 0.5 mm in diameter but 0.04 mm in depth and no rear surface deformation.
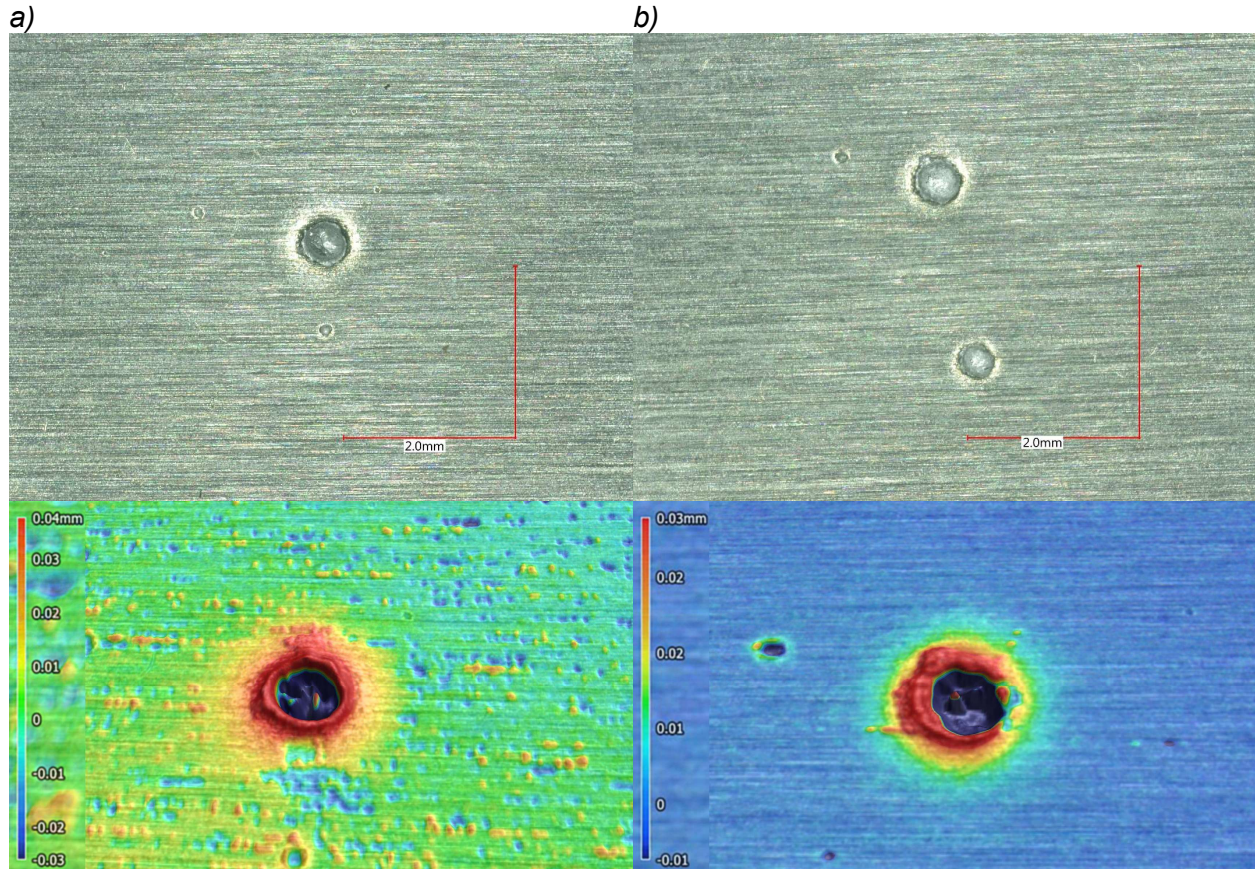
Figure 4 Witness plate images and 2D contours of the most significant craters from a) HITF20358 and b) HIT20357. Images have a scale reference in view, and the contours have the depth color scale in view.

As KM2® Plus 775 is replacing KM2® 705, additional impact speeds have been performed to better characterize 775. HITF20359 considered an impact at 2.02 km/s with a 0.43 mm SS440C projectile. The micrographs for each layer of Kevlar® are shown for HITF20359 in Figure 5. All five layers of the Kevlar® are perforated. The entrance and exit hole of the fifth layer for this shot is difficult to see as the projectile interacted with a single yarn. It is also notable that for each fabric layer there is minimal charring of the Kevlar® fabric.
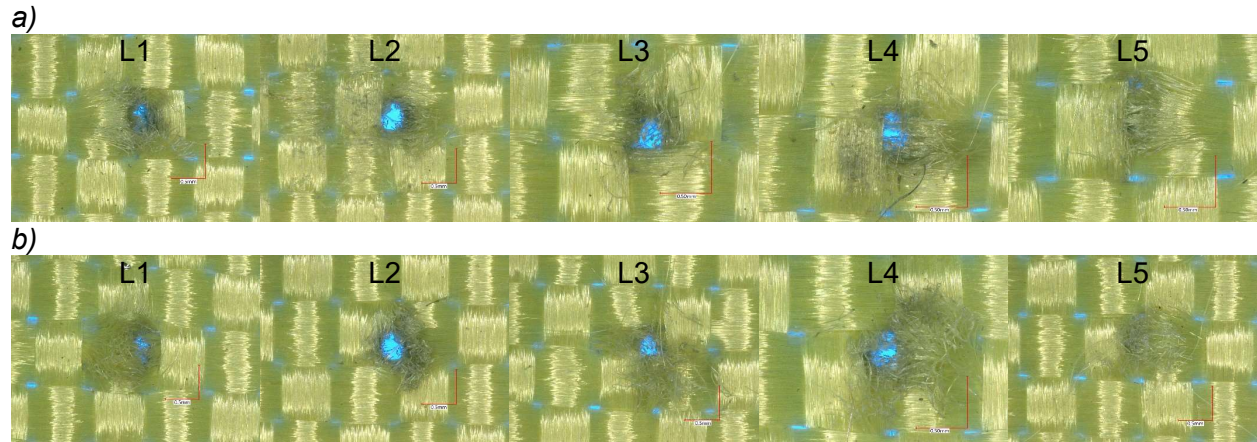
a)

b)

Figure 5 HITF20359 a) front side image of the KM2® Plus 775 layers and b) corresponding back side images. Holes in the fabric are backlit by blue light. Each image from L1 to L5 corresponds to the order of the Kevlar® in the stack. The scale in the images is 0.50 mm.

A third higher impact speed of 4.15 km/s has been considered in HITF20356 with a 0.31 mm SS440C projectile. The micrographs for each layer of Kevlar® are shown in Figure 6. All five layers of the Kevlar® are perforated; additionally, the Kevlar® fabric experienced significant charring through all five layers. The diameter of the damaged areas also indicates that the steel projectile broke up significantly while passing through the Kevlar®.
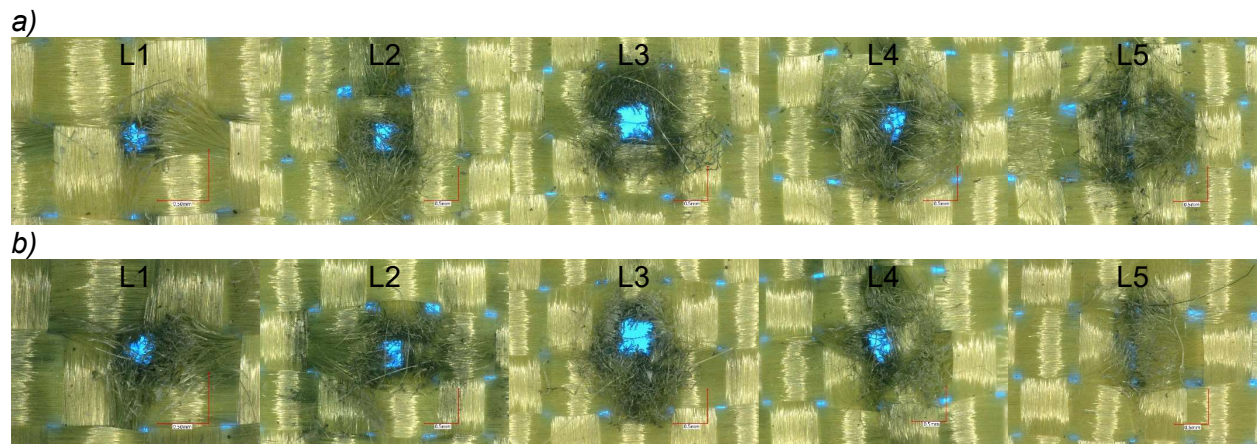
a)

b)

Figure 6 HITF20356 a) front side image of the KM2® Plus 775 layers and b) corresponding back side images. Holes in the fabric are backlit by blue light. Each image from L1 to L5 corresponds to the order of the Kevlar® in the stack. The scale in the images is 0.50 mm.

Examination of the witness plates, Figure 7, shows that the state of the projectile that passed through the Kevlar® in HITF20359 is significantly different than the higher speed projectile from HITF20356. As can be seen in Figure 4a, the projectile made it through the Kevlar® as a single particle and produced a 0.5 mm diameter perforation through the Al2024-T3 witness. In contrast, the impact debris spread across the witness plate in HITF20356 from a projectile fragmentation while passing through the Kevlar® layers. The most significant crater being a 0.4 mm by 0.5 mm elliptical crater with a 0.2 mm deep. This crater induced a 0.04 mm bump on the rear surface of the witness plate.
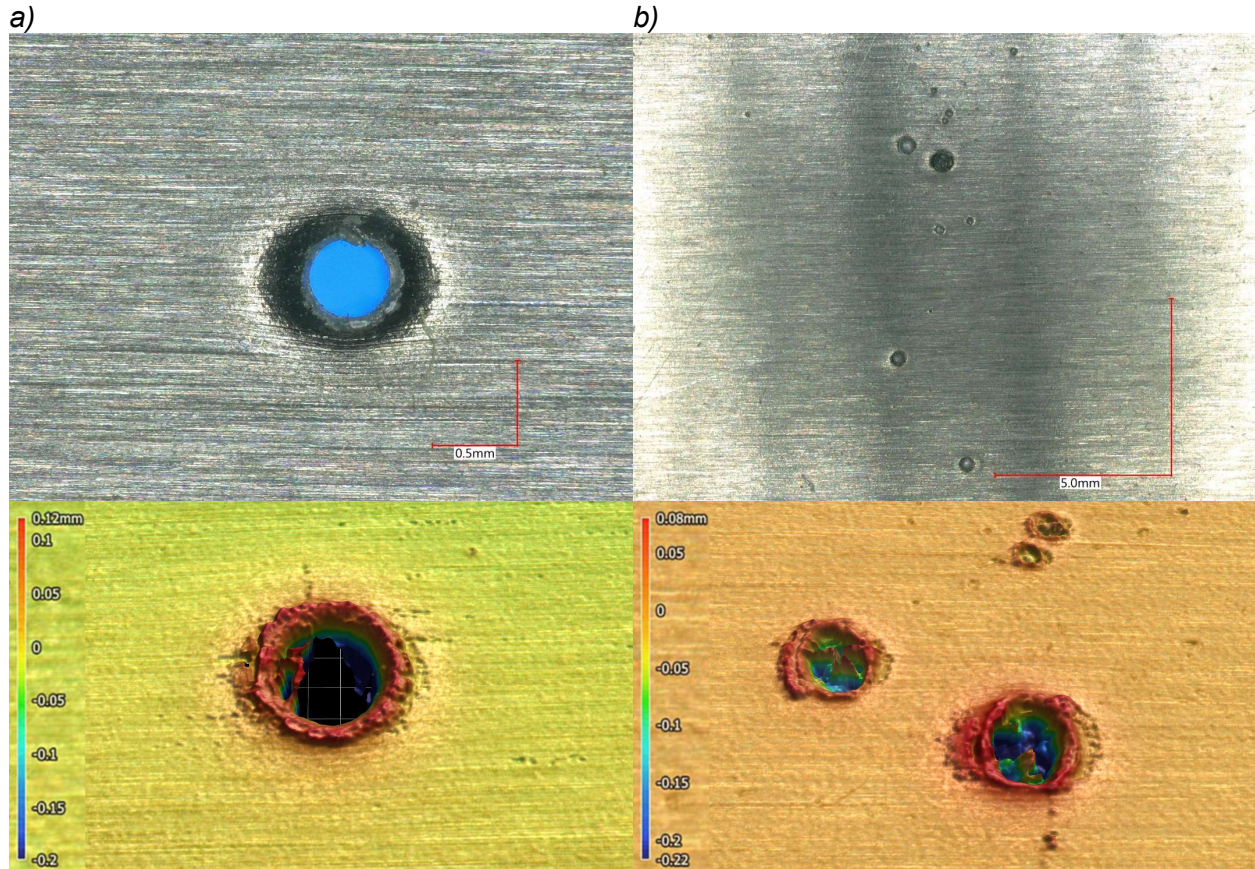
Figure 7 Witness plate images and 2D contours of the most significant craters from a) HITF20359 with a 2.0 mm scale reference in view and b) HITF20356 with a 5.0 mm scale reference in view. The contours have the depth color scale in view. Holes in the plate are backlit by blue light.

These direct-impact experiments are simplistic; however, the nature of Kevlar® complicates even the interpretation of these impact experiments. As can be seen in the micrographs of the Kevlar®, the non-isotropic nature of the weave makes the projectiles path through the fabric layers complicated. As a result of this non-isotropy, fully analyzing these results requires the use of numerical simulations to determine key properties of the two fabric types.

While HITF20356 shows that at impact speeds of approximately 4 km/s the Kevlar® itself is sufficient to start to physically change even steel projectiles, this fracturing/melting is still not to the same level as other materials and requires significantly more mass to accomplish the same breakup. As such, Kevlar® is more commonly used as a subsequent layer to arrest vaporous and small fragments in a double-wall shield. To capture the relative performance of KM2® 705 to KM2® Plus 775 in this role, impact experiments have been performed to quantify the dependence of the material for a relevant MPCV-ESM configuration.

Double-Wall (Whipple) Shield

The MPCV-ESM implementation of Kevlar®, like most implementations of ballistic fabrics, uses Kevlar® as a part of an overall passive-thermal-control, MLI blanket. The enhanced, MLI blanket both thermally insulates the titanium propellant tanks from the aluminum radiator surrounding it, and the blanket also protects the tanks from debris generated during a MMOD impact on the radiator. While the geometry of propellant tanks within the cylindrical radiator of the MPCV-ESM

8

is complicated, the MLI blanket is concentric with the radiator at a constant separation of 10 cm as shown schematically in Figure 8a. This blanket consists of one layer of either KM2® 705 or KM2® Plus 775 fabric fronted by 19 layer MLI that has a mass of 0.035 g/cm^2 and backed by an aluminized Mylar® with Dacron® netting that has a mass of 0.009 g/cm^2. A 2.0 mm Ti6Al4V (Grade 5) witness plate is used to stand in for the propellant tank 22.1 cm behind the 1.3 mm Al6063-T6 radiator surrogate. Like the direct impact targets, the frames holding the fabrics and the aluminum and titanium plates are held in place with threaded rods, washers and locking nuts with a representative target image shown in Figure 8b.
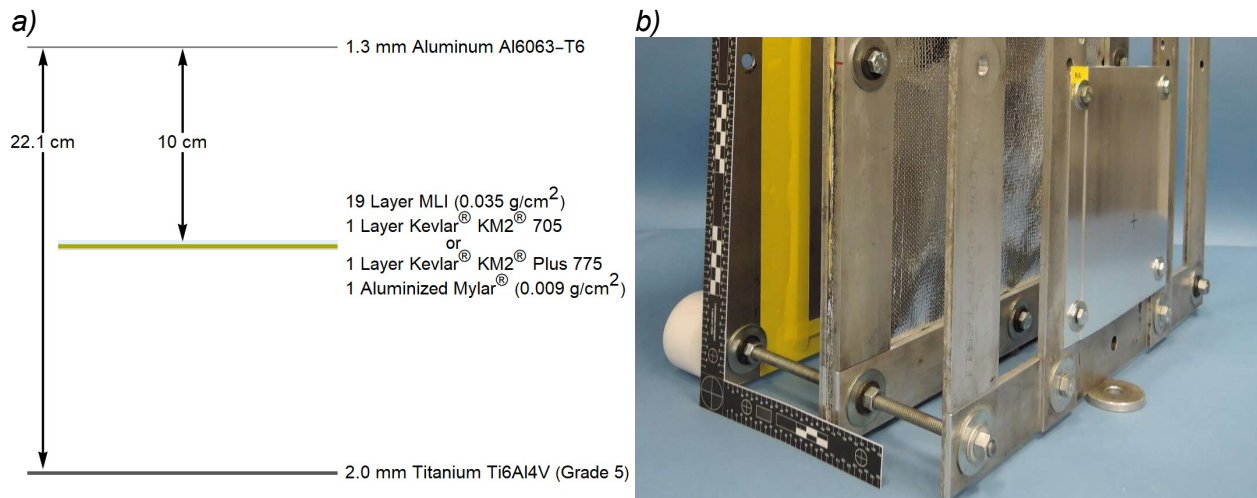

Figure 8 Target images a) scaled representation and b) image of actual target with supporting hardware.

The objective for the double-wall, impact experiments is to quantify the level of ballistic protection afforded to the propellant tanks by the different types of Kevlar®. To this end, an important damage measurement is the depth of the deepest crater in the tank surrogate as a function of various ballistic parameters like projectile material and size and impact conditions like the projectile velocity. This information has been gathered for both KM2® 705 and KM2® Plus 775 fabric enhancements and is given in Table 4.

A total of twenty-one impact experiments using an enhanced MLI blanket with a single KM2® 705 or KM2® Plus 775 performed for MPCV-ESM have been performed. Of those twenty-one impacts, seven used the KM2® 705 and fourteen used the KM2® Plus 775. In this series of experiments, Nylon, Al2017, SS440C and alumina (Al$_2$O$_3$) projectiles have been used to represent low-density debris and icy meteoroids, aluminum debris, high-density debris/ferritic meteoroids, and rocky meteoroids, respectively. The speed is generally around 7 km/s, which is a comfortable maximum speed for the WSTF, two-stage, light-gas-gun. The obliquity is the angle relative to the target's normal vector; therefore, an obliquity of 0° indicates a projectile velocity vector that is straight into the target.

Table 4 Results matrix for ballistic enhancement with single layer of Kevlar® in MPCV-ESM [8, 9]

Test Number	Fabric Type	Projectile Type	Projectile Diameter (cm)	Projectile Mass (g)	Impact Speed (km/s)	Impact Obliquity (°)	Max Ti Crater Depth (mm)
HITF18329	705	Nylon	0.437	0.05002	7.03	0	0.03
HITF18330	705	Nylon	0.755	0.25700	7.01	0	0.60
HITF18331	705	Nylon	0.194	0.00436	6.85	45	0.10
HITF18332	705	Nylon	0.357	0.02717	6.97	45	0.40
HITF18333	705	Nylon	0.276	0.01251	7.27	60	0.09
HITF18334	705	Al2017	0.556	0.25114	6.89	0	0.00
HITF18335	705	SS440C	0.357	0.18261	7.10	0	1.60
HITF20171	775	Nylon	0.437	0.04997	6.94	0	0.09
HITF20172	775	Nylon	0.673	0.18158	6.98	0	0.19
HITF20173	775	Nylon	0.191	0.00413	7.24	45	0.04
HITF20174	775	Al2017	0.699	0.50023	6.96	0	0.08
HITF20175	775	Al_2O_3	0.480	0.22581	6.95	0	0.00
HITF20176	775	SS440C	0.275	0.08387	7.10	0	0.35
HITF20177	775	SS440C	0.237	0.05329	7.05	45	0.49
HITF20189	775	Nylon	0.397	0.03726	7.08	0	0.03
HITF20190	775	Nylon	0.240	0.00829	7.00	45	0.20
HITF20191	775	Al_2O_3	0.605	0.45146	6.97	0	0.11
HITF20192	775	SS440C	0.209	0.03657	7.06	45	0.39
HITF20204	775	Nylon	0.276	0.01248	7.35	60	0.04
HITF20279	775	Nylon	0.240	0.00826	5.17	0	0.06
HITF20280	775	Nylon	0.357	0.02721	7.04	0	0.00

In particular, three Nylon impact conditions have been repeated between KM2® 705 and KM2® Plus 775. These three conditions are all generally at 7 km/s with obliquities of 0° (HITF18329 and HITF20171), 45° (HITF18331 and HITF20173) and 60° (HITF18333 and HITF20204). Close-up micrographs of the deepest craters in the tank surrogate are shown in Figure 9 with those corresponding to the KM2® 705 in Figure 9a and KM2® Plus 775 in Figure 9b. As can be seen in these direct comparisons, the craters are considerably broader when the enhanced MLI uses KM2® Plus 775 rather than KM2® 705. There are small, mixed differences between the maximum depths in the tank surrogates; however, the depths in the Ti6Al4V panels behind the KM2® Plus 775 enhanced MLI are generally lower than the KM2® 705. In particular, the Nylon impacts into KM2® 705 had depths of 0.03, 0.10 and 0.09 mm for the 0°, 45° and 60°, respectively, which compares to 0.09, 0.04 and 0.04 mm for the KM2® Plus 775 for the same obliquities.
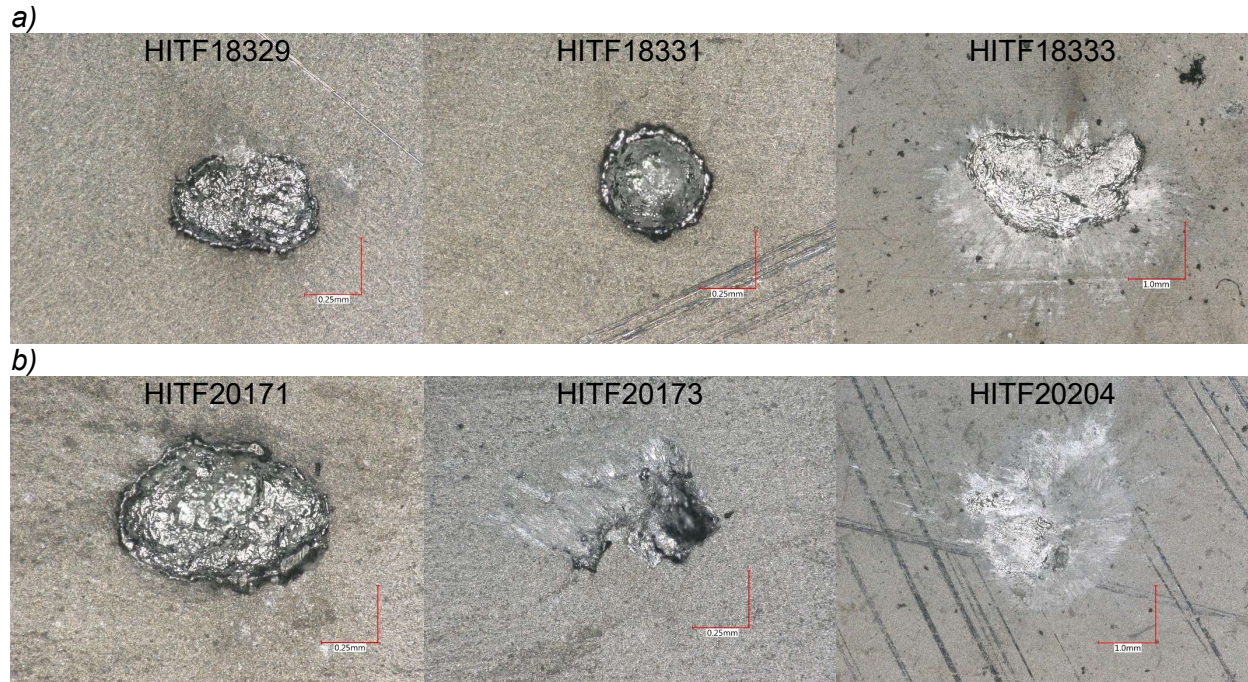
a)

HITF18329 HITF18331 HITF18333

b)

HITF20171 HITF20173 HITF20204

Figure 9 Comparative images from similar impact conditions for a) KM2® 705 and b) KM2® Plus 775. From left-to-right the conditions are 0°, 45° and 60° and approximately 7 km/s.

Discussion

As seen in the direct-impacts and the representative double-wall shield performance assessments, Kevlar®, being a woven fabric, has a complex response to impacts by MMOD like particles. To address this complexity, both numerical simulations to generalize the performance and statistical analysis are used to evaluate the two forms of Kevlar® relative to each fabric type. This section goes over the approach for backing out the dynamic strength for each fabric type from the direct-impacts, and the statistical analysis to relate fabric type to a functional form of critical damage of a titanium structure from the double-wall shield measurements.

Numerical Evaluation of Direct-impacts

The numerical evaluation uses the CTH hydrodynamic simulation tool to explicitly advance the projectile through the Kevlar fabric layers. In the simulations, each of the four direct-impact experiments have been considered. All four of the simulations used a fixed, three-dimensional, cubic mesh with a spatial resolution of 50 µm and have been carried out to 10 µs after the initial impact. The simulation space extends 0.525 cm into each transverse direction from the impact point, and the simulation space extends 0.35 cm below and 0.05 cm above the impact point. This mesh region and duration of simulation is sufficient to contain all of the materials of the impact experiments including the projectiles less the aluminum witness plate.

In the case of numerical simulations, it is possible to reproduce each experiment's projectile passage through the Kevlar® layers and back out material strength. To accomplish this, a fabric model for Kevlar® has been developed as illustrated in Figure 10a where the top of the image is the actual Kevlar® fabric and the bottom is a model of the fabric. The model is constructed of tubes scaled to make the combined weave 0.03 cm in thickness, and transversely scaled to 0.086 cm to match the average width of the Kevlar® yarns, which is the same for both fabric types. The fabric layers have been imported and translated such that the shot line for each of the direct-

11

impact experiments is reproduced as illustrated in Figure 10b from the simulation model of HITF20357.
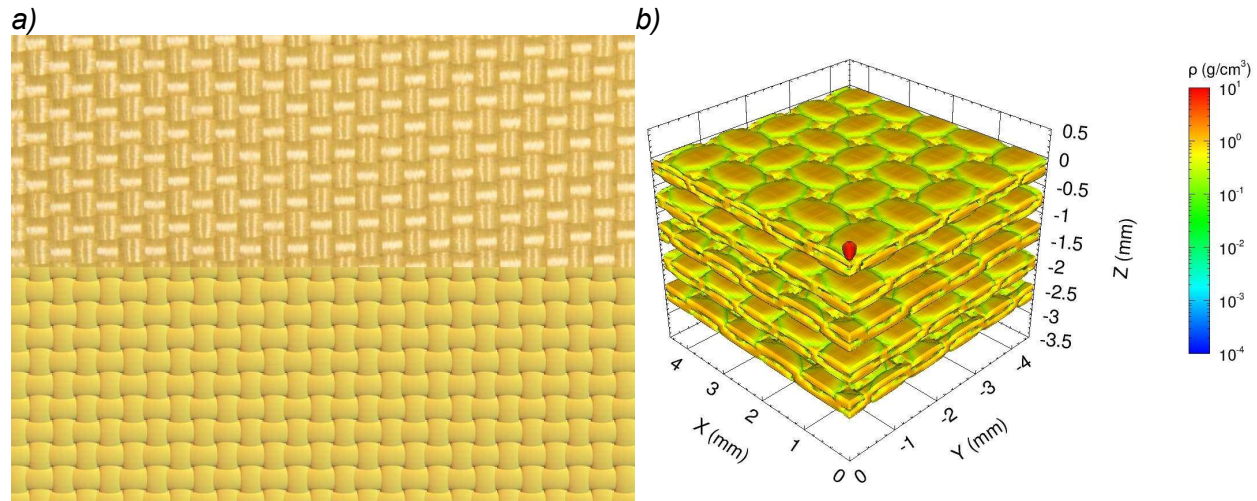
a)

b)

Figure 10 The geometric model used in the numerical simulations of the direct-impact experiments a) comparison of actual KM2® Plus 775 (upper) to the model (lower) and b) simulation configuration of HITF20357 with the five layers of Kevlar®.

The constitutive models, equation-of-state (bulk properties) and strength (deviatoric properties), have been developed for the materials in the simulation using CTH data inputs as much as possible. The steel projectile model used in the simulations is the native iron SESAME equation-of-state (EOS) that is scaled to the molecular weight of SS440C as described in Appendix A. The scaling ratio applies to both the density, which yields a simulated density of 7.675 g/cm^3, and to the internal energy of the material. The strength model used for the SS440C projectile is the Johnson-Cook model as described in Appendix A. Moduli are related to the bulk modulus given by the EOS and the Poisson ratio of 0.28. The model has an initial yield strength without work hardening of 1,180 MPa. Fracture is assumed to occur around the ultimate tensile strength of SS440C of -1,970 MPa. When the local stress inside the cell containing the projectile falls below this fracture stress, void is introduced into the material until the local stress rises to 60% above the fracture stress.

Table 5 Summary of material properties used in the simulations

	Equation-of-State				Deviatoric			
	SESAME Model	Ref (g/cm^3)	Sim (g/cm^3)	Mass (g/cm^2)	Strength Model	Yield (MPa)	Fracture (MPa)	PR
SS440C	Iron SR 1.0257	7.872	7.675	NA	JO	1,180	-1,970	0.28
Kevlar® KM2®	Polyimide	1.414	1.414	0.0241	EPPVM	850	-850	0.24
Kevlar® KM2® Plus	Polyimide Porosity	1.414	1.355	0.0230	EPPVM	950	-950	0.24

The Kevlar® fabrics are also modeled with a SESAME EOS; however, there is not a native EOS for polyamide which makes up Kevlar®, so the polyimide native model is used. The reference density of the polyimide model is 1.414 g/cm^3, which is slightly below the Kevlar® density of 1.44 g/cm^3. The polyimide density of 1.414 g/cm^3 with the fabric geometric model yielded a fabric mass of 0.0241 g/cm^2. As this mass is approximately the mass of the KM2® 705 fabric, the polyimide SESAME EOS has been used without adjustment. As for the KM2® Plus 775, to achieve the lower

fabric mass a porous density of 1.355 g/cm^3 has been used. This density combined with the fabric geometry model yields a mass of 0.0230 g/cm^2. A negligible resistance to full compaction has been assumed.

The deviatoric model has been the objective of this effort. The simplest model of elastic/perfectly-plastic von Mises has been used. This model has no work or strain-rate hardening, and simply assumes linear elastic to yield in pure tension or a factor of square root of three lower than yield in shear. After yield, the material's stress state evolves according to the EOS until reaching the fracture stress. As data for Kevlar® fibers show that the material tends to not have plasticity in pure tension, the fracture stress has been assumed to be the negative of the yield, and the relaxation of tensile (negative) stress is again via void insertion. The Poisson ratio has been maintained at 0.24 for both fiber systems.

The two values have been adjusted together to best reproduce the direct-impact experiments for HITF20358 for KM2® 705 and HITF20357 for KM2® Plus 775. The comparison of the simulations and the observed results are given in Figure 11. In Figure 11a, the experimental images shown in Figure 2a are the background with the simulation results using 850 MPa for the strength of KM2® 705 plotted on top. As can be seen, the simulations closely reproduce the observations, and in particular the simulated damage on the fifth layer is highly representative of the observed damage to this layer. Similarly, the simulated results for KM2® Plus 775 using 950 MPa for the strength and the observed damage in HITF20357 is shown in Figure 11b. Once again the comparison between the simulations and experimental observations are good at each layer of the Kevlar® stack.
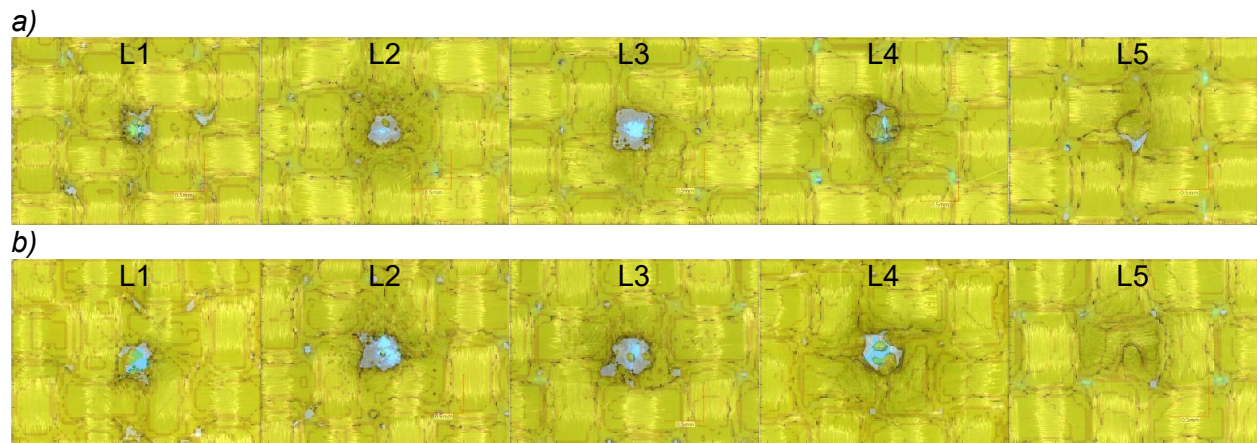
a)

b)

Figure 11 Simulated Kevlar® layer damage combined with the observed damage for a) HITF20358 from Figure2a and b) HITF20357 from Figure3a. Perforation in the simulation is transparent to allow the blue back light to be visible.

The development of the strength has been focused on the direct-impact experiments at approximately 3.5 km/s; however, for the KM2® Plus additional speeds have been considered. The comparison of the simulations and the observed results for these off-speed impacts are given in Figure 12. Figure 12a shows the comparison for the approximately 2 km/s impact with the experimental images set as the background and the simulation results plotted on top. As can be seen, the simulations are reasonably good; however, the predicted perforations from the simulation are a bit larger than the observed damage. The simulated perforation in the fifth layer of Kevlar is 1.0 mm x 0.7 mm, whereas, the observed perforation is 0.8 mm x 0.2 mm. Kevlar® material is pushed back in the simulation at the time the simulation stopped, and it is possible given much longer simulation times the material would partially reclose the hole.
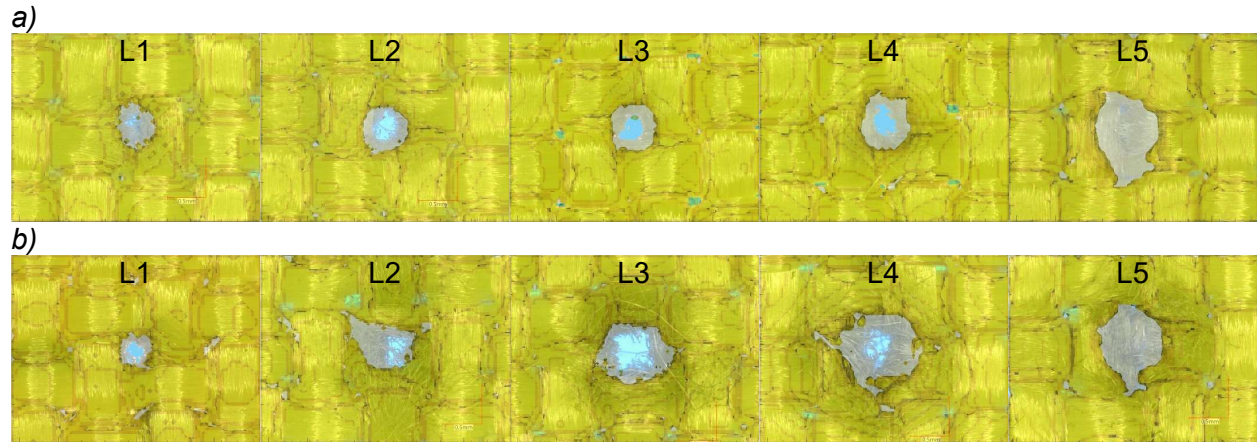
a)

L1 L2 L3 L4 L5

b)

L1 L2 L3 L4 L5

Figure 12 Simulated Kevlar® layer damage combined with the observed damage for a) HITF20359 from Figure 5a and b) HITF20356 from Figure 6a. Perforation in the simulation is transparent to allow the back light to be visible.

Figure 12b shows the comparison for the 4.15 km/s impact. As before, the experimental images are set as the background, and the simulation results are plotted over the background. As can be seen, the simulations caught much of the extensive damage that is seen in Figure 6, but as with the simulation of HITF20359 these shots are well above the critical projectile and Kevlar® material is pushed back. The simulated perforation is 1.1 mm x 0.8 mm while the observed perforation is 1.3 mm x 0.3 mm. As with HITF20359, it is possible given much longer simulation times the material would partially reclose the hole.

While additional experimental work is necessary to get a better description of the uncertainty in the dynamic strength of the Kevlar fabric types, from this limited dataset it is anticipated that the minimum dynamic strength of the KM2® 705 yarn is 850±50 MPa, and the minimum dynamic strength of the KM2® Plus 775 yarn is 950±50 MPa. This means that the relative fabric-to-fabric dynamic strength improvement of KM2® Plus 775 to KM2® 705 is 12±9%. Additionally, KM2® Plus 775 is about 3.6±0.7% lighter than KM2® 705 resulting in even higher mass performance with the upgraded fabric.

Statistical Analysis of Double-Wall (Whipple) Shield Experiments

Direct-impact property measurements have yielded a glimpse into the potential of an improvement from the migration from KM2® 705 to KM2® Plus 775; however, a more direct, albeit less generalized, observation is possible for the specific shield system, shown in Figure 1, that has been characterized for MPCV-ESM. As noted in Table 4, twenty-one impact experiments have been performed in this effort and all but one of them has been performed at approximately 7 km/s. As such, the small differences in the impact speed are neglected and the maximum crater depth as reported in Table 4 are shown for each shot in Figure 13 as a function of the type and diameter of the projectile that made the crater, and the results are further separated by type of Kevlar® and impact obliquity for each type of projectile.

In Figure 13a, the twelve impact experiments to characterize the MPCV-ESM Kevlar® enhanced MLI system are shown where shots that had a single KM2® 705 layer as the enhancement are shown with circles, and shots that had a single KM2® Plus 775 layer as the enhancement are shown with a plus sign. The shots are segregated by impact obliquity using color where 0° to normal impacts are blue, 45° to normal impacts are orange and 60° to normal impacts are green. This same approach of showing separating the type of Kevlar® in the enhanced MLI and obliquity

are repeated for the other three types of projectiles considered: SS440C in Figure 13b, Al2017 in Figure 13c and Al₂O₃ in Figure 13d; although, as can be seen in the figures the amount of effort put into the other materials decreased significantly compared to Nylon.
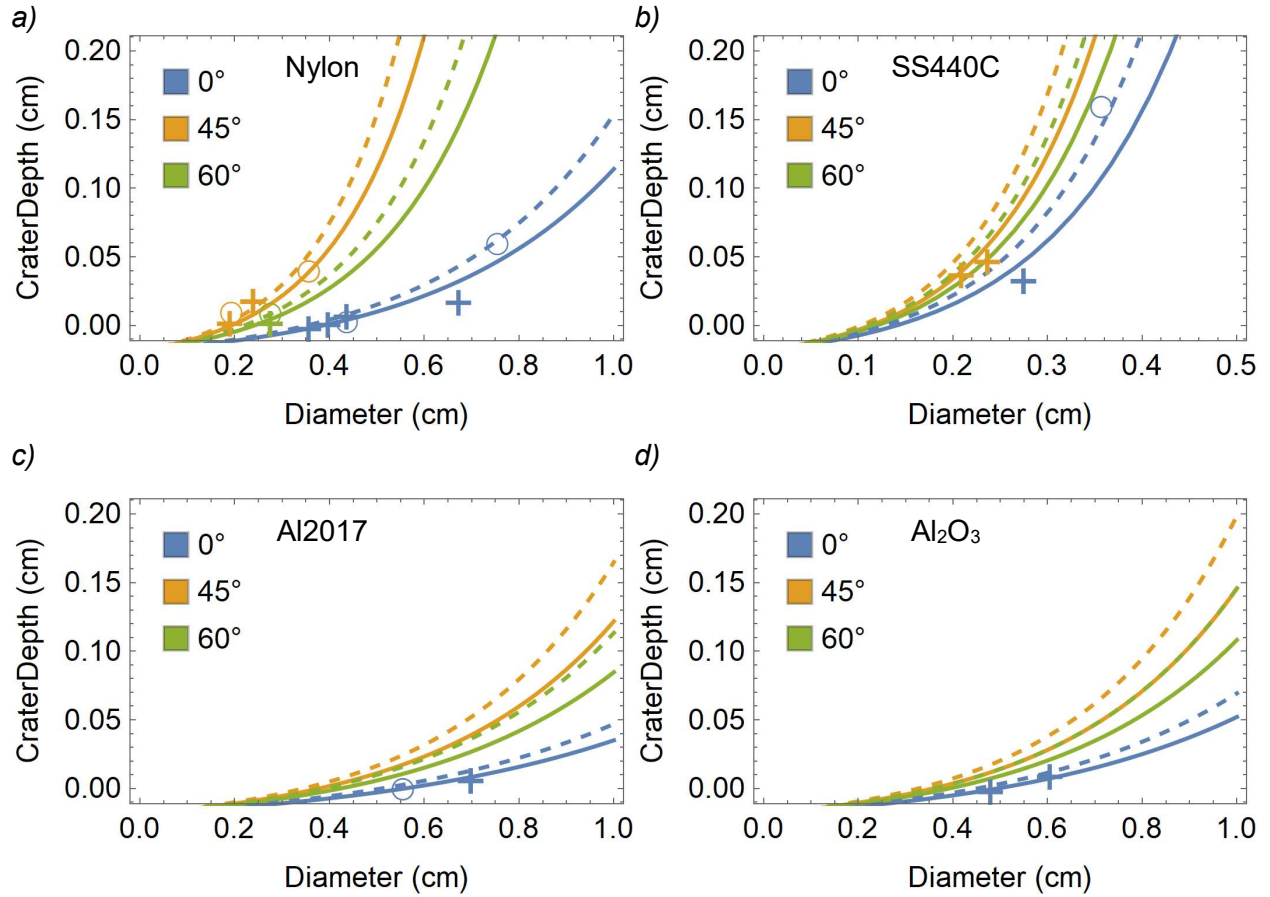

Figure 13 Experimental maximum crater depth evidence gathered for the MPCV-ESM against a) Nylon, b) SS440C, c) Al2017 and d) Al₂O₃ projectile impacts. Shots with KM2® 705 as the enhancement are shown with circles, and those with KM2® Plus 775 are shown with plus signs. Color is used to identify the obliquity that the projectile impacted the target. In addition to the impact data, the nonlinear fitted model is shown with the data and color coded the same where the dashed line is for KM2® 705 and the solid line for KM2® Plus 775.

The disperse dataset has been consolidated by fitting a nonlinear model for the maximum crater depth, P, to the projectile type (represented by density of the projectile), projectile diameter and impact obliquity. The relational form of the model is given by,

$$P[\rho_p, \theta_i, D_p] = \bar{P}\left(Exp\left[\frac{D_p}{\left(\frac{\bar{D}}{1+\delta}\right)\left(1 - \frac{Sin^2[2\,\theta_i]}{2}\left(\frac{\rho_N}{\rho_p}\right)^Q\right)\left(\frac{\rho_N}{\rho_p}\right)^{R\,\rho_p+S}} - 1\right] - 1\right), \qquad (1)$$

where ρ_p, θ_i and D_p are the independent variables of projectile density, impact obliquity and projectile diameter, respectively. As Nylon is the principal component of the accumulated database, the modeling has been done in reference to Nylon and its density, ρ_N. The fitting

15

parameter estimates, standard error of estimate and the t-Statistic for the estimates are given in Figure 14a for the parameters of Eqn. 1.

While the model is *ad hoc*, some of the parameters have common meanings. By inspection, it can be seen that the denominator in the exponential function is the equation for the critical diameter for the onset of cratering in the MPCV-ESM shield. Further, the ratio of the first parameter, $\bar{P}$, to that critical diameter is the linear growth rate of the crater on the critical surface. The second parameter, $\bar{D}$, is the mean Nylon critical diameter for normal impacts for both Kevlar® fabric types. Both $\bar{P}$ and $\bar{D}$ have units of centimeters in this dataset.

a)

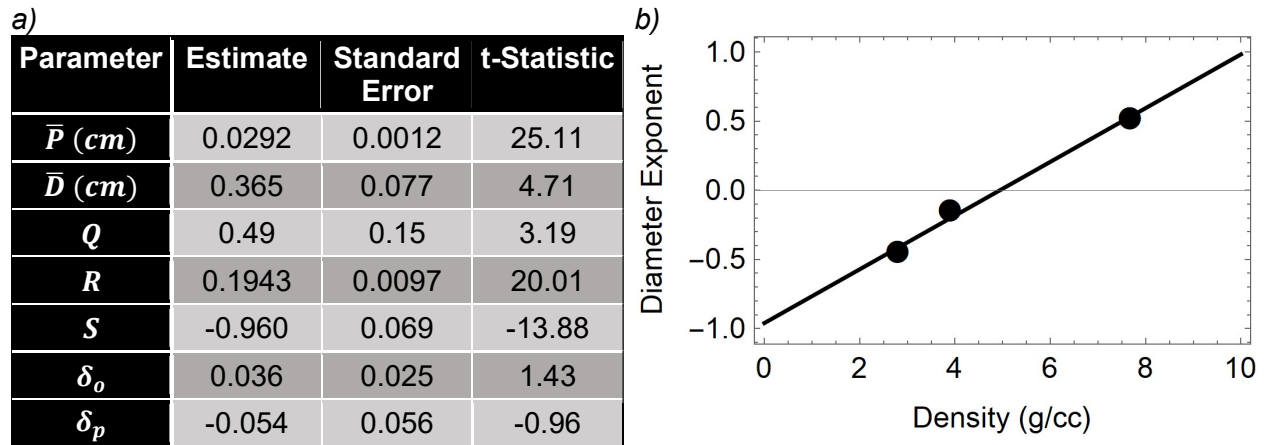| Parameter	Estimate	Standard Error	t-Statistic
$\bar{P}$ (cm)	0.0292	0.0012	25.11
$\bar{D}$ (cm)	0.365	0.077	4.71
Q	0.49	0.15	3.19
R	0.1943	0.0097	20.01
S	-0.960	0.069	-13.88
δ_o	0.036	0.025	1.43
δ_p	-0.054	0.056	-0.96

b)

Figure 14 Model inputs including a) the fitting parameters necessary for model usage and b) the fitting approach used for extrapolating away from Nylon for critical particle size that addresses Al2017 (2.8 g/cm³), Al₂O₃ (3.9 g/cm³) and SS440C (7.68 g/cm³).

The exponent Q modifies the dependence of obliquity for the critical particle size. This exponent is derived from those materials where oblique shots have been performed, which is limited to Nylon and SS440C, so the quality of the parameter estimation is low with a large standard error and poor t-Statistic. While the limited data has affected the estimate, the two materials that data is available represent the lowest and highest densities anticipated to be encountered in operational environments, which means that this term is interpolating rather than extrapolating in this model.

The exponent relating the critical diameter to the projectile material for normal impacts can be compared to all three non-Nylon materials. The exponents are 0.49±0.15 for SS440C, -0.437±0.052 for Al2017 and -0.135±0.025 for Al₂O₃. These three values can be used on their own, but as shown in Figure 14b, they are modeled well by a simple linear function, which is defined in Figure 14a by R and S.

Together Eqn. 1 and the first five parameters in Figure 14a yield the mean performance with the two fabrics assumed equivalent. The difference between the two fabrics are modeled by δ_o for KM2® 705 and δ_p for KM2® Plus 775, which has been accomplished by fitting the fabrics individually to their dataset while all other values are left at the mean. This complete model is shown in Figure 13 as the curves accompanying the experimental data where the dashed curves correspond to KM2® 705 and the solid curves to KM2® Plus 775. As can be seen, the model reproduces the available dataset well. To further illustrate this, the residuals from the data to the fitted model are shown in Figure 15 as a function of the three independent variables: projectile material, projectile diameter and impact obliquity. As can be seen, errors in prediction are less than 0.2 mm and generally within 0.1 mm. The coefficient of determination for the fit of is 0.969.
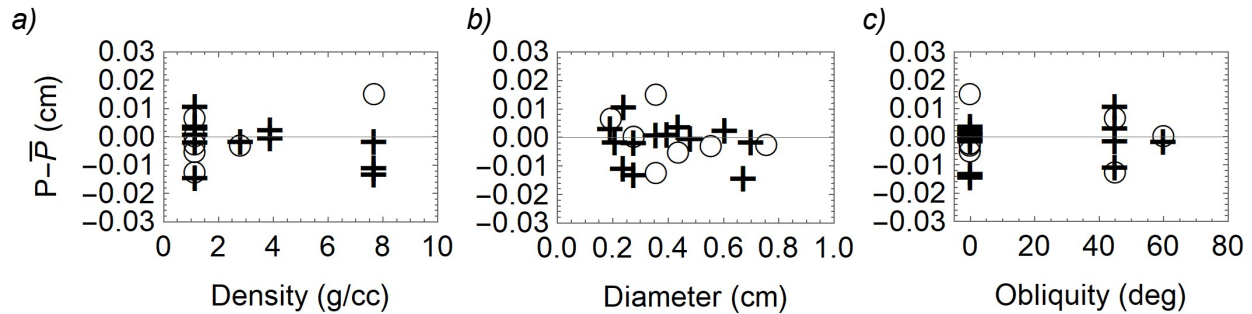
Figure 15 Target images a) scaled representation and b) image of actual target with supporting hardware. Shots with KM2® 705 as the enhancement are shown with circles, and those with KM2® Plus 775 are shown with plus signs.

While overall the fit is of high quality, extrapolations could be suffering from limited size of the foundational dataset and should be performed with caution. Extrapolations back to the onset of cratering, though, have high confidence. Using the model to account for all projectile types and impact obliquities, the onset of cratering is 9.5±6.1% higher for KM2® Plus 775 as compared to its predecessor KM2® 705, which is in-line with the direct-impact estimates.

Conclusions

In this paper, two methods for examining the relative ballistic performance of the new KM2® Plus 775 fabric as compared to KM2® 705 fabric, which has been widely adopted by NASA systems designers to enhance protection of critical components. The first method discussed is direct impacts into the two Kevlar fabrics by a known projectile at representative conditions for debris cloud particles. This method consisted of two phases. The first phase consisted of impact experiments on the fabrics near the ballistic limit of fabrics, and the second phase consisted of numerically backing out the relative dynamic strength of the fabrics. From these examinations, it has been found that KM2® Plus does in fact improve the ballistic performance as an MLI enhancement with a predicted improvement of 12±9% between the two fabrics.

The second method discussed considered the two different fabrics as an enhancement to an MLI blanket in a representative shield system. This approach looked at a broad range of projectile types, projectile diameters and impact obliquities and their effect on resultant craters in a titanium (Ti6Al4V) witness plate behind the enhanced MLI blanket for each material. While an expected scatter resulted from this comparison, when all of the conditions are considered the KM2® Plus 775 outperformed the KM2® 705 by 9.5±6.1%.

This work has developed material models for numerical simulations to further extrapolate the types of uses for Kevlar® and will allow exploration of material performance to speeds that are currently outside the achievable speeds of ground-based accelerators. Additional direct-impact experiments would help narrow the uncertainty bounds of Kevlar® material properties, and additional double-wall shield experiments would improve extrapolations to more damage for risk assessments that use Kevlar® enhanced MLI blankets. With those additional needs noted, this work demonstrates that the forced transition from KM2® 705 to KM2® Plus 775 is very likely acceptable for MMOD shield system applications, and it is especially acceptable based on mass performance.

References

[1] DuPont, "Kevlar aramid fiber: technical guide," DuPont, Richmond, VA, 2017.

[2] M. R. Roenbeck, E. J. Sandoz-Rosado, J. Cline, V. Wu, P. Moy, M. Afshari, D. Reichert, S. R. Lustig and K. E. Strawhecker, "Probing the internal sturctures of Kevlar fibers and their impacts on mechanical performance," *Polymer,* vol. 128, pp. 200-210, 2017.

[3] E. L. Christiansen, "Meteoroid/Debris shielding, NASA TP-2003-210788," National Technical Information Service, Springfield, VA, 2005.

[4] DuPont, "Kevlar KM2 Plus," DuPont, [Online]. Available: https://www.pp.dupont.com/products/kevlar-km2-plus.html. [Accessed 26 May 2021].

[5] M. Smith, D. Craig, N. Herrmann, E. Mahoney, J. Krezel, N. McIntyre and K. Goodliff, "The Artemis Program: an Overview of NASA's Activities to Return Humans to the Moon," *2020 IEEE Aerospace Conference,* no. doi: 10.1109/AERO47225.2020.9172323, pp. 1-10, 2020.

[6] P. Berthe, A. P. Over, M. Gronowski and B. Richard, "Orion European Service Module (ESM) development, integration and qualification status," *2018 AIAA SPACE and Astronautics Forum and Exposition,* no. doi: 10.2514/6.2018-5146, pp. 1-10, 2018.

[7] R. J. McCandless, E. L. Christiansen, B. A. Davis, D. M. Lear and J. E. Miller, "Kevlar KM2/KM2+ property measurement HVI test program (Unpublished)," NASA Johnson Space Center, Houston, TX, 2021.

[8] B. A. Davis, J. E. Miller, K. D. Deighton, D. M. Lear and E. L. Christiansen, "MPCV ESM RA mass reduction and research HVI test program (Unpublished)," NASA Johnson Space Center, Houston, TX, 2021.

[9] B. A. Davis, E. L. Christiansen, K. D. Deighton, D. M. Lear and J. E. Miller, "ESM MDPS single layer Kevlar mass reduction HVI test program (Unpublished)," NASA Johnson Space Center, Houston, TX, 2021.

[10] Hexcel, "Aramid fabric construction data," in *HexForce reinforcements: technical fabrics handbook*, Seguin, TX, Hexcel, 2010, p. 104.

[11] JPS Composite Materials, "Technical reference handbook," in *Technical references*, Anderson, SC, Handy & Harman Company, 2017, p. 67.

[12] Hexcel, "705 Aramid and high performance fabrics product data," Hexcel Schwebel, Anderson, SC.

[13] J. Cline, V. Wu and P. Moy, "Assessment of the tensile properties for single fibers," US Army Research Laboratory (ARL-TR-8299), Aberdeen Proving Ground, MD, 2018.

Appendix A

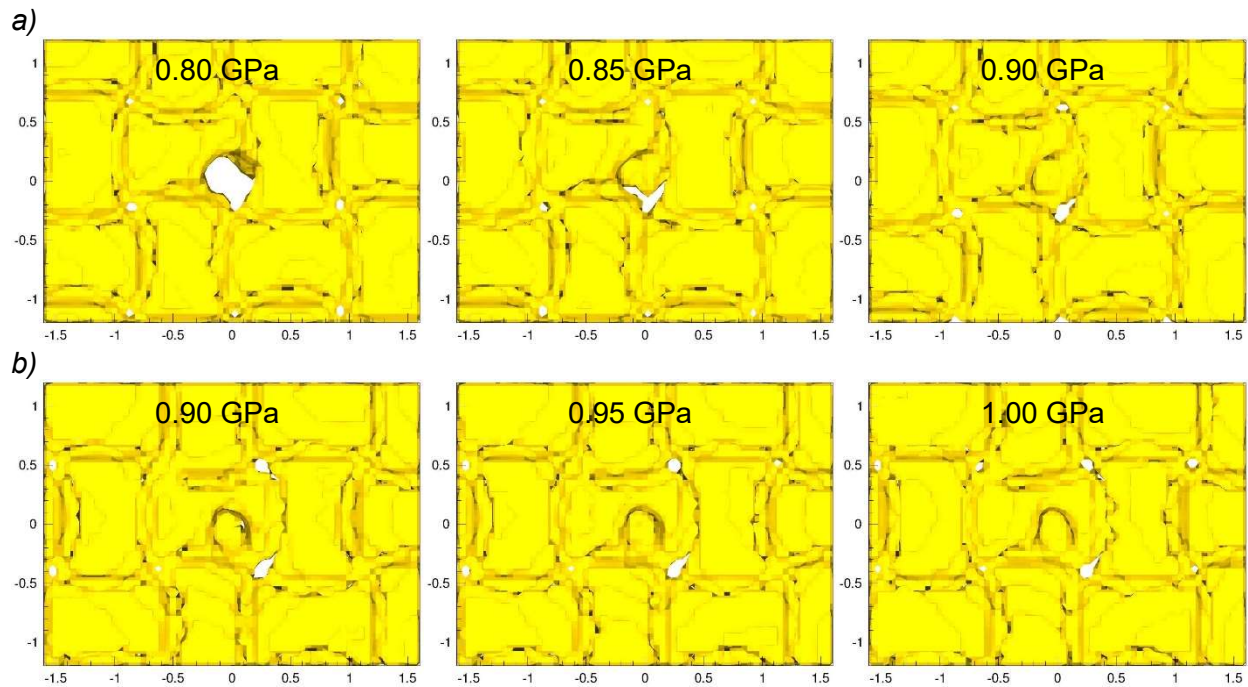| SS440C	Mat Analysis	Wt. Fraction	Element Mass (AMU)	Weighted Mass (AMU)
C	0.95-1.20%	0.01075	12.0107	0.1291
Cr	16.0-18.0%	0.17	51.9961	8.8393
Si	1.00%	0.01	28.0855	0.2809
Mn	1.0% Max	0.005	54.9381	0.2747
P	0.040%	0.0004	30.9738	0.0124
SS	0.030%	0.0003	32.065	0.0096
Mo	0.075%	0.00075	95.94	0.0720
Fe	80.28%	0.8028	55.845	44.8324

Appendix B

Figure 16 Comparative images for three different strengths for a) HITF20358 and b) HITF20357.